A&A 526, A89 (2011)
DOI: 10.1051/0004-6361/201015801

Astronomy & Astrophysics

The fundamental parameters of the roAp star γ Equulei

K. Perraut[1], I. Brandão[2], D. Mourard[3], M. Cunha[2], Ph. Bério[3], D. Bonneau[3], O. Chesneau[3], J. M. Clausse[3], O. Delaa[3], A. Marcotto[3], A. Roussel[3], A. Spang[3], Ph. Stee[3], I. Tallon-Bosc[4], H. McAlister[5,6], T. ten Brummelaar[6], J. Sturmann[6], L. Sturmann[6], N. Turner[6], C. Farrington[6], and P. J. Goldfinger[6]

[1] Laboratoire d'Astrophysique de Grenoble (LAOG), Université Joseph-Fourier, UMR 5571 CNRS, BP 53, 38041 Grenoble Cedex 09, France
e-mail: karine.perraut@obs.ujf-grenoble.fr
[2] Centro de astrofísica e Faculdade de Ciências, Universidade do Porto, Portugal
[3] Laboratoire Fizeau, OCA/UNS/CNRS UMR6525, Parc Valrose, 06108 Nice Cedex 2, France
[4] Université de Lyon, 69003 Lyon, France; Université Lyon 1, Observatoire de Lyon, 9 avenue Charles André, 69230 Saint Genis Laval; CNRS, UMR 5574, Centre de Recherche Astrophysique de Lyon; Ecole Normale Supérieure, 69007 Lyon, France
[5] Georgia State University, PO Box 3969, Atlanta GA 30302-3969, USA
[6] CHARA Array, Mount Wilson Observatory, 91023 Mount Wilson CA, USA

Received 21 September 2010 / Accepted 3 November 2010

ABSTRACT

Context. A precise comparison of the predicted and observed locations of stars in the H-R diagram is needed when testing stellar interior theoretical models. For doing this, one must rely on accurate, observed stellar fundamental parameters (mass, radius, luminosity, and abundances).
Aims. We determine the angular diameter of the rapidly oscillating Ap star, γ Equ, and derive its fundamental parameters from this value.
Methods. We observed γ Equ with the visible spectro-interferometer VEGA installed on the optical CHARA interferometric array, and derived both the uniform-disk angular diameter and the limb-darkened diameter from the calibrated squared visibility. We then determined the luminosity and the effective temperature of the star from the whole energy flux distribution, the parallax, and the angular diameter.
Results. We obtained a limb-darkened angular diameter of 0.564 ± 0.017 mas and deduced a radius of $R = 2.20 \pm 0.12\ R_\odot$. Without considering the multiple nature of the system, we derived a bolometric flux of $(3.12 \pm 0.21) \times 10^{-7}$ erg cm^{-2} s^{-1} and an effective temperature of 7364 ± 235 K, which is below the previously determined effective temperature. Under the same conditions we found a luminosity of $L = 12.8 \pm 1.4\ L_\odot$. When the contribution of the closest companion to the bolometric flux is considered, we found that the effective temperature and luminosity of the primary star can reach ~100 K and ~0.8 $L_\odot$ lower than the values mentioned above.
Conclusions. For the first time, and thanks to the unique capabilities of VEGA, we managed to constrain the angular diameter of a star as small as 0.564 mas with an accuracy of about 3% and to derive its fundamental parameters. In particular the new values of the radius and effective temperature should bring further constraints on the asteroseismic modeling of the star.

Key words. methods: observational – techniques: high angular resolution – techniques: interferometric – stars: individual: γEqu – stars: fundamental parameters

1. Introduction

Rapidly oscillating Ap (roAp) stars are chemically peculiar main-sequence stars that are characterized by strong and large-scale organized magnetic fields (typically of several kG, and up to 24 kG), abundance inhomogeneities leading to spotted surfaces, small rotational speeds, and pulsations with periods of a few minutes (see, Kochukhov 2009; Cunha 2007, for recent reviews). The roAp stars are bright, pulsate with large amplitudes and in high radial orders. Thus they are particularly well-suited to asteroseismic campaigns, and they contribute in a unique way to our understanding of the structure and evolution of stars. However, to put constraints on the interior chemical composition, the mixing length parameter, and the amount of convective overshooting, asteroseismic data should be combined with high-precision stellar radii (Cunha et al. 2003, 2007). This radius is generally estimated from the star's luminosity and effective temperature. But systematic errors are likely to be present in this determination owing to the abnormal surface layers of the Ap stars. This well known fact has been corroborated by seismic data on roAp stars (Matthews et al. 1999), and compromises all asteroseismic results for this class of pulsators. Using long-baseline interferometry to provide accurate angular diameters appears to be a promising approach to overcome the difficulties in deriving accurate global parameters of roAp stars, but is also very challenging because of their small angular size. In fact, except for α Cir, whose diameter is about 1 millisecond of arc (mas) (Bruntt et al. 2008), all roAp stars have angular diameters smaller than 1 mas. Such a small scale can be resolved only with optical or near-infrared interferometry. This was confirmed again recently by the interferometric study of the second largest (in angular size) roAp star known, namely β CrB (Bruntt et al. 2010).

One of the brightest objects in the class of roAp stars is γ Equ (HD201601; A9p; $m_V = 4.7$; $\pi_P = 27.55 \pm 0.62$ mas, van Leeuwen 2007; $v \sin i \sim 10$ km s^{-1}, Uesugi & Fukuda 1970) with a period of about 12.3 min (Martinez et al. 1996) in brightness, as well as in radial velocity. Despite photometry and spectroscopy of its oscillations obtained over the past 25 years, the

Table 1. Journal of γ Equ observations on July 29 and on August 3 and 5, 2008.

Date	UT (h)	Star	B (m)	PA (°)
2008-07-29	5.59	HD 195810	78.9	106.6
2008-07-29	6.08	γ Equ	76.2	106.4
2008-07-29	6.41	HD 195810	92.3	101.9
2008-08-03	8.64	HD 195810	107.3	93.0
2008-08-03	8.98	γ Equ	107.8	93.8
2008-08-03	9.31	HD 195810	103.7	91.0
2008-08-05	7.68	HD 195810	107.3	108.8
2008-08-05	8.14	γ Equ	106.7	95.8
2008-08-05	8.63	HD 195810	106.9	92.6

Table 2. Calibrated squared visibilities of γ Equ, where each point corresponds to the average on the 60 blocks of 500 frames.

UT (h)	B (m)	λ_0 (nm)	V^2
6.08	76.1	745.0	0.84 ± 0.02
6.08	76.2	582.5	0.72 ± 0.02
8.98	107.6	640.0	0.62 ± 0.04
8.14	106.7	640.0	0.61 ± 0.05

pulsation frequency spectrum of γ Equ has remained poorly understood. High-precision photometry with the MOST satellite has led to unique mode identifications based on a best model (Gruberbauer et al. 2008) using a mass of 1.74 ± 0.03 $M_\odot$, an effective temperature of $\log T_{\rm eff} = 3.882 \pm 0.011$, and a luminosity of $\log L/L_\odot = 1.10 \pm 0.03$ (Kochukhov & Bagnulo 2006). Ryabchikova et al. (2002) consider the following stellar parameters ($T_{\rm eff}$ = 7700 K, $\log g$ = 4.2, [M/H] = +0.5) to compute synthetic spectra and present the evidence for abundance stratification in the atmosphere of γ Equ: Ca, Cr, Fe, Ba, Si, Na all seem to be overabundant in deeper atmospheric layers, but normal to underabundant in the upper layers. According to the authors, this agrees well with diffusion theory for Ca and Cr, developed for cool magnetic stars with a weak mass loss of about 2.5×10^{-15} $M_\odot$/yr. Pr and Nd from the rare earth elements have an opposite profile since their abundance is more than 6 dex higher in the upper layers than in the deeper atmospheric ones. Such abundance inhomogeneities clearly lead to a patchy surface, a redistribution of the stellar flux, and a complex atmospheric structure, resulting in biased photometric and spectroscopic determinations of the effective temperature.

Guided by these considerations, we observed γ Equ with a spectro-interferometer operating at optical wavelengths, the VEGA spectrograph (Mourard et al. 2009) installed at the CHARA Array (ten Brummelaar et al. 2005). The unique combination of the visible spectral range of VEGA and the long baselines of CHARA allowed us to record accurate squared visibilities at high spatial frequencies (Sect. 2). To derive the fundamental parameters of γ Equ, calibrated spectra were processed to estimate the bolometric flux and to determine the effective temperature (Sect. 3). Finally, we can set the star γ Equ in the HR diagram and discuss the derived fundamental parameters (Sect. 4).

2. Interferometric observations and data processing

Data were collected at the CHARA Array with the VEGA spectropolarimeter recording spectrally dispersed fringes at visible wavelengths thanks to two photon-counting detectors. Two telescopes were combined on the W1W2 baseline. Observations were performed between 570 and 750 nm (according to the detector) at the medium spectral resolution of VEGA (R = 5000). Observations of γ Equ were sandwiched between those of a nearby calibration star (HD 195810). The observation log is given in Table 1.

Each set of data was composed of observations following a calibrator-star-calibrator sequence, with 10 files of 3000 short exposures of 15 ms per observation. Each data set was processed in 60 files of 500 short exposures using the C_1 estimator and the VEGA data reduction pipeline detailed in Mourard et al. (2009). The spectral separation between the two detectors is fixed by the optical design and equals about 170 nm in the medium spectral resolution. The red detector was centered on 750 nm on July 29 and on 640 nm on August 3 and 5. The blue detector was centered on 590 nm on July, 29 and on 470 nm on August 3 and 5. The bluer the wavelength, the more stringent the requirements on seeing. As a consequence the blue data on August 3 and 5 did not have a sufficient signal-to-noise ratio and squared visibilities could not be processed. All the squared visibilities are calibrated using an uniform-disk angular diameter of 0.29 ± 0.02 mas in the V and R bands for the calibrator HD 195810. This value is determined from the limb-darkened angular diameter provided by SearchCal[1] (Table 2).

The target γ Equ is the brightest component of a multiple system. The closest component lies at 1.25″ ± 0.04″ and has a magnitude difference with the primary star of Δm = 4 and a position angle of PA = 264.6° ± 1.3° (Fabricius et al. 2002). The entrance slit of the spectrograph (height = 4″ and width = 0.2″ for these observations) will affect the transmission of the companion flux. Taking into account the seeing during the observations (about 1″), the field rotation during the hour angle range of our observations ([−30°; 0°]), and the position angle of the companion, we determined the throughput efficiency of the VEGA spectrograph slit for this companion. This efficiency varies from 10% for the longer baselines (around 107 m) to 30% for the smaller ones (around 80 m). We used the Visibility Modeling Tool (VMT)[2] to build a composite model including the companion of γ Equ. For the longer baselines, the resulting modulation in the visibility is below 2%, which is 3 or 4 times below our accuracy on squared visibilities. We thus neglected the influence of the companion and interpreted our visibility data points in terms of angular diameter (Fig. 1). We performed model fitting with LITpro[3]. This fitting engine is based on a modified Levenberg-Marquardt algorithm combined with the trust regions method (Tallon-Bosc et al. 2008). The software provides a user-expandable set of geometrical elementary models of the object, combinable as building blocks. The fit of the visibility curve versus spatial frequency leads to a uniform-disk angular diameter of 0.540 ± 0.016 mas for γ Equ. We used the tables of Diaz-Cordoves et al. (1995) to determine the linear limb-darkening coefficient in the R band for $4.0 \leq \log g \leq 4.5$ and 7500 K $\leq T_{\rm eff} \leq$ 7750 K. By fixing this limb-darkening coefficient, LITPRO provides a limb-darkened angular diameter in the R band of $\theta_{\rm LD} = 0.564 \pm 0.017$ mas with a reduced χ^2 of 0.37.

[1] http://www.jmmc.fr/searchcal_page.htm
[2] http://www.nexsciweb.ipc.caltech.edu/vmt/vmtWeb
[3] http://www.jmmc.fr/litpro_page.htm

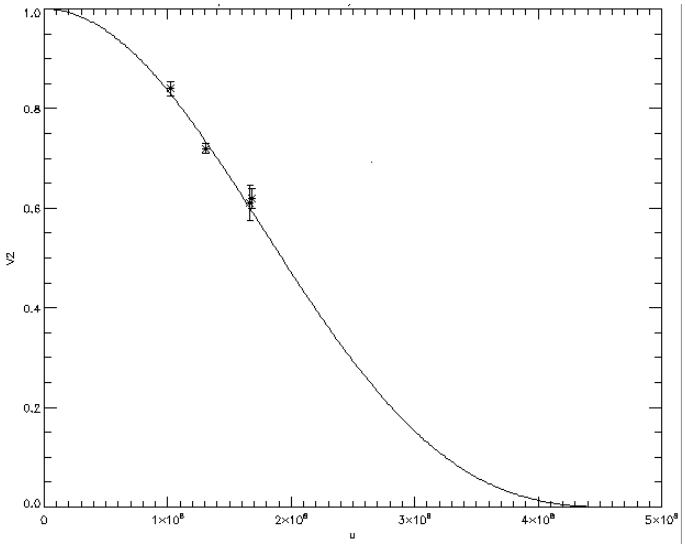

Fig. 1. Squared visibility versus spatial frequency u for γ Equ obtained with the VEGA observations. The solid line represents the uniform-disk best model.

3. Bolometric flux and effective temperature

The effective temperature, $T_{\rm eff}$, of a star can be obtained through the relation,

$$\sigma T_{\rm eff}^4 = 4 f_{\rm bol}/\theta_{\rm LD}^2, \quad (1)$$

where σ stands for the Stefan-Boltzmann constant (5.67×10^{-5} erg cm^{-2} s^{-1} K^{-4}), $\theta_{\rm LD}$ for the limb-darkened angular diameter, and $f_{\rm bol}$ is the star's bolometric flux given by

$$f_{\rm bol} = \int_0^\infty F(\lambda) {\rm d}\lambda. \quad (2)$$

The effective temperature of γ Equ can thus be computed if we know its angular diameter and its bolometric flux. The angular diameter of γ Equ was derived in Sect. 2. To compute the bolometric flux we need a single spectrum that covers the whole wavelength range. This spectrum was obtained by combining photometric and spectroscopic data of γ Equ available in the literature, together with ATLAS9 Kurucz models, as explained below.

3.1. Data

We collected two rebinned high-resolution spectra (R = 18 000 at λ = 1400 Å, R = 13 000 at λ = 2600 Å) from the Sky Survey Telescope obtained at the *IUE* "Newly Extracted Spectra" (INES) data archive[4], covering the wavelength range [1850 Å; 3350 Å]. The two spectra were obtained with the Long Wavelength Prime camera and the large aperture of 10″ × 20″ (Table 3). Based on the quality flag listed in the IUE spectra (Garhart et al. 1997), we removed all bad pixels from the data and also the points with negative flux. The mean of the two spectra was then computed to obtain one single spectrum of γ Equ in the range 1850 Å < λ < 3350 Å.

We collected two spectra for γ Equ in the visible, one from Burnashev (1985), which is a spectrum from Kharitonov et al. (1978) reduced to the uniform spectrophotometric system of the "Chilean Catalogue", and one from Kharitonov et al. (1988). We verified that the latter was in better agreement with the Johnson (Morel & Magnenat 1978) and the Geneva (Rufener 1988) photometry than the other spectrum. To convert from Johnson and Geneva magnitudes to fluxes we used the calibrations given by Johnson (1966) and Rufener & Nicolet (1988), respectively.

For the infrared, we collected the photometric data available in the literature. The calibrated observational photometric fluxes that we considered in this study are given in Table 4.

[4] http://sdc.laeff.inta.es/cgi-ines/IUEdbsMY

Table 3. UV spectra obtained with IUE.

Image Number	Date	Starting time (UT)	Exposure time (s)
06874	08/10/1985	18:55:04	599.531
09159	23/09/1986	20:41:13	539.730

Table 4. Calibrated photometric infrared fluxes for γ Equ.

Band	$\lambda_{\rm eff}$ (Å)	Flux ($\times 10^{-12}$ erg cm^{-2} s^{-1} Å^{-1})	Source	Calibration
I	9000	15.53	1	a
J	12 500	5.949	2	b
H	16 500	2.420	2	b
K	22 000	0.912	2	b
L	36 000	0.140	2	b
M	48 000	0.0512	2	b
J	12 350	6.090	3	c
H	16 620	2.584	3	c
K	21 590	1.067	3	c

Notes. Source references: (1) Morel & Magnenat (1978); (2) Groote & Kaufmann (1983); (3) Cutri et al. (2003). Calibration references: (a) Johnson (1966); (b) Wamsteker (1981); (c) Cohen et al. (2003).

3.2. Determination of $f_{\rm bol}$ and $T_{\rm eff}$

The spectrum of γ Equ was obtained by combining the averaged IUE spectrum between 1854 Å and 3220 Å, the Kharitonov's (1988) spectrum from 3225 Å to 7375 Å, and for wavelengths λ < 1854 Å and λ > 7390 Å we considered two cases. (1) We used the synthetic spectrum for the Kurucz model that best fitted both the star's spectrum in the visible and the star's photometry in the infrared. (2) We performed a linear extrapolation between 506 Å and 1854 Å, considering zero flux at 506 Å, a second linear interpolation to the infrared fluxes between 7390 Å and 48 000 Å, and a third linear extrapolation from 48 000 Å and 1.6×10^6 Å considering zero flux at 1.6×10^6 Å. In case (1), when searching for the best Kurucz model, we intentionally disregarded the data in the UV, because Kurucz models are particularly unsuitable for modeling that region of the spectra of roAp stars. To find the Kurucz model that best fitted the data in the visible and infrared, we ran a grid of models, with different effective temperatures, surface gravities, and metallicities. Since Kurucz models needed to be calibrated (they give the flux of the star, not the value observed on Earth), we tried two different calibrations: (i) the star's magnitude in the V band, m_V, and (ii) the relation $(R/d)^2$, where R is the radius and d the distance to the star. For the $R/d = \theta/2$ we used the limb-darkened angular diameter $\theta_{\rm LD}$ determined in the previous section. The final spectra obtained for γ Equ with the two different calibration methods and with the interpolation method are plotted in Fig. 2. The bolometric flux, $f_{\rm bol}$, was then computed from the integral of the spectrum

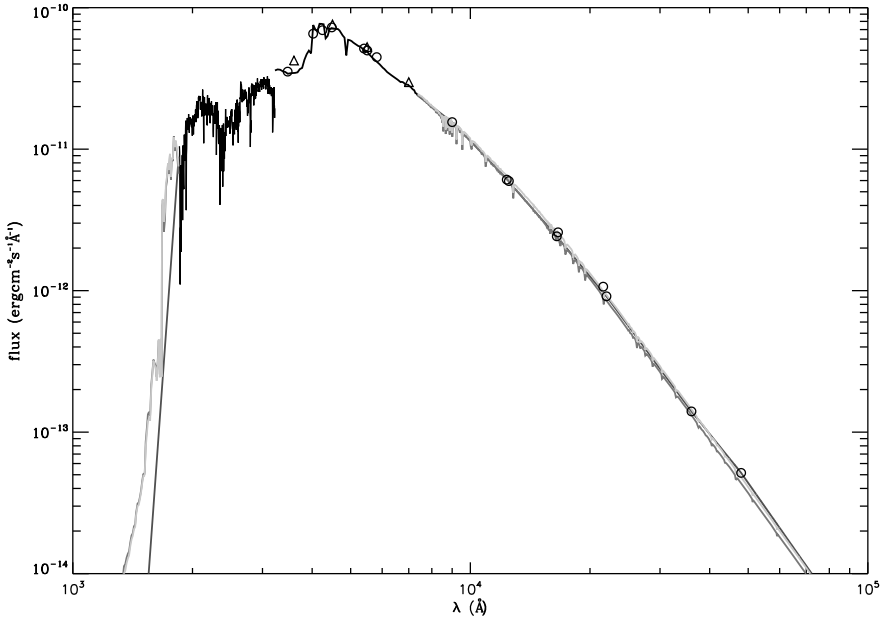

Fig. 2. The whole spectrum obtained for γ Equ. Black line corresponds to the average of the IUE spectra and to the Kharitonov et al. (1988)'s spectrum. For wavelengths $\lambda < 1854$ Å and $\lambda > 7390$ Å, the figure shows the curve obtained using the interpolation method (dark gray line), the Kurucz model that best fits the spectroscopy in the visible and the photometry in the infrared when models are calibrated with the star's magnitude m_V (gray line) and when models are calibrated with the relation $(R/d)^2$ (light gray line). The Geneva and infrared photometry from Table 4 (circles) and Johnson *UBVRI* photometry (triangles) are overplotted to the spectrum.

Table 5. Bolometric flux $f_{\rm bol}$ and effective temperature $T_{\rm eff}$ obtained for γ Equ, using three different methods (see text for details).

Calibration method	$f_{\rm bol}$ (erg cm^{-2} s^{-1})	$T_{\rm eff}$ (K)
m_V	$(3.09 \pm 0.20) \times 10^{-7}$	7351 ± 229
$(R/d)^2$	$(3.15 \pm 0.21) \times 10^{-7}$	7381 ± 234
Interpolation	$(3.11 \pm 0.21) \times 10^{-7}$	7361 ± 235

of the star through Eq. (2), and the effective temperature, $T_{\rm eff}$, was determined using Eq. (1) (Table 5).

The uncertainties in the three values of the bolometric flux given in Table 5 were estimated by considering an uncertainty of 10% on the total flux from the combined IUE spectrum (González-Riestra et al. 2001), an uncertainty of 4% on the total flux of the low-resolution spectrum from Kharitonov et al. (1988), an uncertainty of 20% on the total flux derived from the Kurucz model, and an uncertainty of 20% on the total flux derived from the interpolation. The last two are somewhat arbitrary. Our attitude was one of being conservative enough to guarantee that the uncertainty in the total flux was not underestimated due to the difficulty in establishing these two values. The corresponding absolute errors were then combined to derive the errors in the flux, which are shown in Table 5. Combining these with the uncertainty in the angular diameter, we derived the uncertainty in the individual values of the effective temperature. As a final result we take the mean of the three values and consider the uncertainty to be the largest of the three uncertainties. Thus, the flux and effective temperature adopted for γ Equ are $(3.12 \pm 0.21) \times 10^{-7}$ erg cm^{-2} s^{-1} and 7364 ± 235 K. If, instead, we took for the effective temperature an uncertainty such as to enclose the three uncertainties, the result would be $T_{\rm eff} = 7364 \pm 250$ K.

3.3. Contamination by the companion star

Since γ Equ is a multiple system and the distance between the primary (hereafter γ Equ A) and the secondary (hereafter γ Equ B) is 1.25″, the bolometric flux of γ Equ determined in Sect. 3 contains the contribution of both components. Given its magnitude, one may anticipate that the contribution of γ Equ B to the total flux will be small. Although the data available in the literature for this component is very limited, we used them to estimate the impact of γ Equ B's contribution on our determination of the effective temperature of γ Equ A.

We collected the magnitudes $m_B = 9.85 \pm 0.03$ and $m_V = 8.69 \pm 0.03$ of γ Equ B from Fabricius et al. (2002) and determined a value for its effective temperature using the color-$T_{\rm eff}$ calibration from Ramírez & Meléndez (2005). This assumed three different arbitrary values and uncertainties for the metallicity, namely -0.4 ± 0.5, 0 ± 0.5, and 0.4 ± 0.5 dex. The values found for the effective temperature were $T_{\rm eff} = 4570$, 4686, and 4833 K, respectively, with an uncertainty of ±40 K (Ramírez & Meléndez 2005). The metallicity, the effective temperature, and the absolute V-band magnitude were used to estimate $\log g$, using theoretical isochrones from Girardi et al. (2000)[5]. For the three values of metallicities and $T_{\rm eff}$ mentioned above, we found $\log g = 4.58$, 4.53, and 4.51, respectively. With these parameters we computed three Kurucz models and calibrated each of them in three different ways: (i) using the $H_{\rm P} = 9.054 \pm 0.127$ mag (Perryman et al. 1997), (ii) using the m_B magnitude, and (iii) using the m_V magnitude. To convert from Hipparcos/Tycho magnitudes into fluxes, we used the zero points from Bessel & Castelli (private communication). The maximum flux found for γ Equ B through the procedure described above was 0.19×10^{-7} erg cm^{-2} s^{-1}, which corresponds to 6% of the total flux. This implies that the effective temperature of γ Equ A determined in the previous section may be in excess by up to 111 K due to the contamination introduced by this companion star.

4. Discussion

4.1. Position in the HR-diagram

We derive the radius of γ Equ thanks to the formula

$$\theta_{\rm LD} = 9.305 * R/d, \quad (3)$$

[5] http://stev.oapd.inaf.it/cgi-bin/param

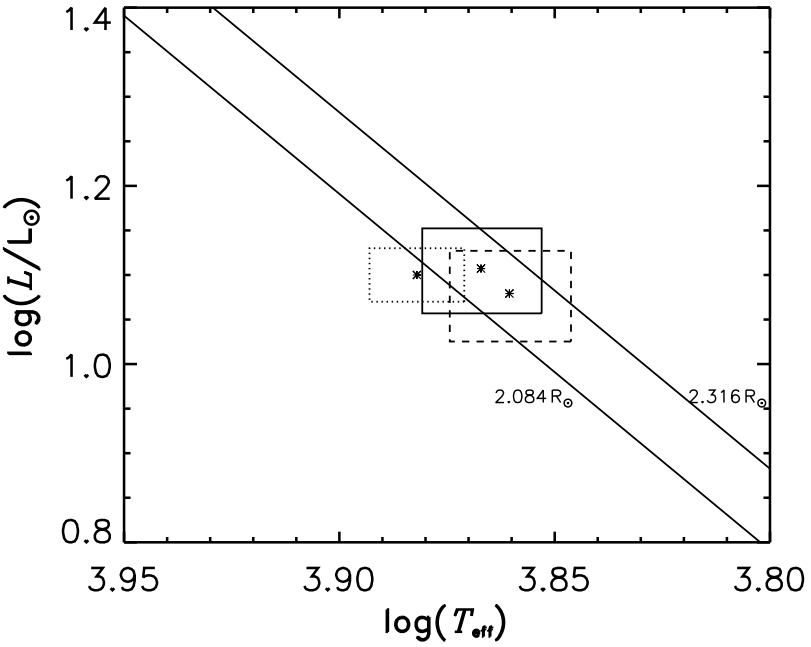

Fig. 3. The position of γ Equ in the Hertzsprung-Russell diagram. The constraints on the fundamental parameters are indicated by the 1σ-error box (log $T_{\rm eff}$, log $(L/L_{\odot})$) and the diagonal lines (radius). The box in solid lines corresponds to the results derived when ignoring the companion star. The box in dashed lines corresponds to the results derived after subtracting from the total bolometric flux the maximum contribution expected from the companion (see text for details). The box in dotted lines corresponds to the fundamental parameters derived by Kochukhov & Bagnulo (2006) and used by Gruberbauer et al. (2008) in the asteroseismic modelling of γ Equ.

where $\theta_{\rm LD}$ stands for the limb-darkened angular diameter (in mas), R for the stellar radius (in solar radius, $R_{\odot}$), and d for the distance (in parsec). We obtain $R = 2.20 \pm 0.12\ R_{\odot}$.

We use the bolometric flux $f_{\rm bol}$ and the parallax $\pi_{\rm P}$ to determine the γ Equ's luminosity from the relation

$$L = 4\pi f_{\rm bol} \frac{C^2}{{\pi_{\rm P}}^2}, \tag{4}$$

where C stands for the conversion factor from parsecs to meters. We obtain $L/L_{\odot} = 12.8 \pm 1.4$ and can set γ Equ in the HR diagram (Fig. 3).

Recently, seismic data of γ Equ obtained with the Canadian-led satellite MOST have been modeled by Gruberbauer et al. (2008) based on the fundamental parameters coming from Kochukhov & Bagnulo (2006) and using a grid of pulsation models that include the effect of the magnetic field. Comparing the HR diagram error box considered by these authors (in dotted line in Fig. 3) and our error boxes shows that the regions are considerably different. In fact, even if we do not account for the contribution of the companion, we obtain a lower effective temperature with log $T_{\rm eff} = 3.867 \pm 0.014$ to be compared to log $T_{\rm eff} = 3.882 \pm 0.011$ from Gruberbauer et al. (2008). This discrepancy between the uncertainty regions increases if the companion contribution is taken into account. In that case, the overlap between the two regions is very small.

For luminosity, our calculation shows that for γ Equ (as well as for α Cir) the contributions of the uncertainties in the bolometric flux and parallax to the uncertainty in $L/L_{\odot}$ are comparable. This is quite different from the results obtained by Kochukhov & Bagnulo (2006), who find that the dominant contribution to the uncertainty in $L/L_{\odot}$ comes from the parallax. The authors mention that the bolometric flux adopted in their work is for normal stars. When dealing with peculiar stars, like Ap stars, it may be more adequate to properly compute the bolometric flux. However, it is precisely the difficulty of obtaining the full spectrum of the star that increases the uncertainty in the computed bolometric flux and, hence, in the luminosity and effective temperature. That is illustrated well by the following fact: if the somewhat arbitrary 20% uncertainties adopted in our work for the total fluxes derived from the Kurucz model and from the interpolation, were replaced by 5% uncertainties, we would obtain formal uncertainties in $L/L_{\odot}$ and $T_{\rm eff}$ comparable and smaller, respectively, to those quoted by Kochukhov & Bagnulo (2006).

4.2. Bias due to stellar features

We used the whole spectral energy density to determine the bolometric flux. We then deduced the effective temperature from this bolometric flux and the angular diameter. The determination of the angular diameter is based on visibility measurements that are directly linked to the Fourier transform of the object intensity distribution. For a single circular star, the visibility curve as a function of spatial frequency B/λ (where B stands for the interferometric baseline and λ for the operating wavelength) is related to the first Bessel function, and contains an ever decreasing series of lobes, separated by nulls, as one observes with an increasing angular resolution. As a rule of thumb, the first lobe of the visibility curve is only sensitive to the size of the object. As an example, for a star whose angular diameter equals 0.56 mas like γ Equ (see Fig. 1), the difference in squared visibility between a uniform-disk and a limb-darkened one is on the order of 0.5% in the first lobe. The following lobes are sensitive to limb darkening and atmospheric structure but consist of very low visibilities. Finally, departure from circular symmetry (due to stellar spots, from instance) requires either interferometric imaging by more than two telescopes or measurement close to zero. As a consequence, our interferometric data collected in the first part of the first lobe are only sensitive to the size of the target and cannot be used to study the potential complex structure of the atmosphere.

5. Conclusion

With the help of the unique capabilities of VEGA/CHARA, we present an accurate measurement of the limb-darkened angular diameter of a target as small as 0.564 ± 0.017 mas. In combination with our estimate of the bolometric flux based on the whole spectral energy density, we determined the effective temperature of γ Equ A. Without considering the contribution of the closest companion star (γ Equ B) to the bolometric flux, we found an effective temperature 7364 ± 235 K, which is below the previously determined effective temperature. An estimate of that contribution leads to the conclusion that the above value may still be in excess by up to about 110 K, which further increases the discrepancy between the literature values for the effective temperature of γ Equ A and the value derived here. The impact on the seismic analysis of considering the new values of the radius and effective temperature should be considered in a future modeling of this star.

More generally, this study illustrates the advantages of optical long-baseline interferometry for providing direct and accurate angular diameter measurements and motivates observations of other main-sequence stars to constrain their evolutionary state and their internal structures. Within this context, the operation of VEGA in the visible is very complementary to the similar interferometric studies performed in the infrared range since it allows study of spectral types ranging from B to late-M and thus opens a new window on the early spectral types (Mourard et al. 2009).

Another promising approach would be to use longer interferometric baselines to be sensitive to the stellar spots and constrain the stellar surface features.

Acknowledgements. VEGA is a collaboration between CHARA and OCA/LAOG/CRAL/LESIA that has been supported by the French programs PNPS and ASHRA, by INSU, and by the Région PACA. The project has obviously benefited from the strong support of the OCA and CHARA technical teams. The CHARA Array is operated with support from the National Science Foundation through grant AST-0908253, the W. M. Keck Foundation, the NASA Exoplanet Science Institute, and from Georgia State University. This work was partially supported by the projects PTDC/CTE-AST/098754/2008 and PTDC/CTE-AST/66181/2006, and the grant SFRH/BD/41213/2007 funded by FCT/MCTES, Portugal. M.C. is supported by a Ciência 2007 contract, funded by FCT/MCTES (Portugal) and POPH/FSE (EC). This research made use of the SearchCal and LITPRO services of the Jean-Marie Mariotti Center, and of CDS Astronomical Databases SIMBAD and VIZIER.

References

Allen, C. W. 1973, 3rd ed. (London: University of London, Athlone Press)
Bruntt, H., North, J. R., Cunha, M. S., et al. 2008, MNRAS, 386, 2039
Bruntt, H., Kervella, P., Mérand, A., et al. 2010, A&A, 512, 55
Burnashev, V. I. 1985, Abastumanskaya Astrofiz. Obs., Byull, 59, 83
Cohen, M., Wheaton, W. A., & Megeath, S. T. 2003, AJ, 126, 1090
Cunha, M. S. 2007, CoAst, 150, 48
Cunha, M. S., Fernandes, J. M., & Monteiro, M. P. 2003, MNRAS, 343, 831
Cunha, M. S., Aerts, C., Christensen-Dalsgaard, J., et al. 2007, A&ARv, 14, 217
Cutri, R. M., Skrutskie, M. F., van Dyk, S., et al. 2003, 2MASS all sky catalogue of point sources
Diaz-Cordoves, J., Claret, A., & Gimenez, A. 1995, A&AS, 110, 329
Fabricius, C., Høg, E., Makarov, V. V., Mason, B. D., Wycoff, G. L., & Urban, S. E. 2002, A&A, 384, 180
Garhart, M. P., Smith, M. A., Turnrose, B. E., Levay, K. L., & Thompson, R. W. 1997, IUE NASA Newsletter, 57, 1
Girardi, L., Bressan, A., Bertelli, G., & Chiosi, C. 2000, VizieR Online Data Catalog, 414, 10371
González-Riestra, R., Cassatella, A., & Wamsteker, W. 2001, A&A, 373, 730
Groote, D., & Kaufmann, J. P. 1983, A&AS, 53, 91
Gruberbauer, M., Saio, H., Huber, D., et al. 2008, A&A, 480, 223
Hubrig, S., Nesvacil, N., Schöller, M., et al. 2005, A&A, 440, L37
Johnson, H. L. 1966, ARA&A, 4, 193
Kharitonov, A. V., Tereshchenko, V. M., & Kniazeva, L. N., 1978, Svodnyi spektrofotometricheskii katalog zvezd, A Compiled Spectrophotometric Catalog of Stars (Alma Ata: Nauka)
Kharitonov, A. V., Tereshchenko, V. M., & Knyazeva, L. N. 1988, The spectrophotometric catalogue of stars. Book of reference, ed. A. V. Kharitonov, et al., ISBN 5-628-00165-1
Kochukhov, O. 2009, CoAst, 159, 61
Kochukhov, O., & Bagnulo, S. 2006, A&A, 450, 763
Kurtz, D. W., Elkin, V. G., Cunha, M. S., et al. 2006, MNRAS, 372, 286
Matthews, J. M., Kurtz, D. W., & Martinez, P. 1999, ApJ, 511, 422
Martinez, P., Weiss, W. W., Nelson, M. J., et al. 1996, MNRAS, 282, 243
Morel, M., & Magnenat, P. 1978, A&AS, 34, 477
Mourard, D., Clausse, J. M., Marcotto, A., et al. 2009, A&A, 508, 1073
Perryman, M. A. C., Lindegren, L., Kovalevsky, J., et al. 1997, A&A, 323, L49
Ramírez, I., & Meléndez, J. 2005, ApJ, 626, 465
Ryabchikova, T., Piskunov, N., Kochukhov, O., et al. 2002, A&A, 384, 545
Rufener, F. 1988, Sauverny: Observatoire de Geneve
Rufener, F., & Nicolet, B. 1988, A&A, 206, 357
ten Brummelaar, T. A., McAlister, H. A., Ridgway, S. T., et al. 2005, ApJ 628, 453
Tallon-Bosc, I., Tallon, M., Thiébaut, E., et al. 2008, SPIE, 7013, 44
Uesugi, A., & Fukuda, I. 1970, Catalog of rotational velocities of the stars
van Leeuwen, F. 2007, A&A, 474, 653
Wamsteker, W. 1981, A&A, 97, 329
Worley, C. E., & Douglass, G. G. 1996, The Washington Visual Double Star Catalog, 1996.0